





Nuclear magnetic quadrupole moment of ^{175}Lu and parity-violating polarization degree of levels in $^{175}\text{Lu OH}^+$

Igor Kurchavov ^{1,*} Daniel Maison,^{1,†} Leonid Skripnikov ^{1,2,‡} Matt Grau ^{3,§} and Alexander Petrov ^{1,2,¶}

¹*Petersburg Nuclear Physics Institute named by B.P. Konstantinov of National Research Center “Kurchatov Institute” (NRC “Kurchatov Institute” - PNPI), 1 Orlova roscha mcr., Gatchina, 188300 Leningrad region, Russia*

²*Saint Petersburg State University, 7/9 Universitetskaya nab., St. Petersburg, 199034 Russia*

³*Department of Physics, Old Dominion University, Norfolk, Virginia 23529, USA*



(Received 5 September 2023; accepted 1 November 2023; published 16 November 2023)

A calculation is performed of the parity-violating polarizations in the external electric field, which are associated with the electron electric dipole moment ($e\text{EDM}$) and magnetic quadrupole moment (MQM) of the ^{175}Lu nucleus, as well as the determination of the rovibrational structure for the $^{175}\text{Lu OH}^+$ cation. Beyond the bending of the molecule, the slight effect of the stretching of the distance between Lu and OH is taken into account. This study is required for the preparation of the experiment and for the extraction of the $e\text{EDM}$ and MQM values of ^{175}Lu from future measurements.

DOI: [10.1103/PhysRevA.108.052815](https://doi.org/10.1103/PhysRevA.108.052815)

I. INTRODUCTION

The pursuit of understanding the fundamental symmetries governing the laws of physics has been a central focus in the field of theoretical and experimental physics. Among these symmetries, the invariance with respect to charge conjugation (\mathcal{C}), spatial parity (\mathcal{P}), and time reversion (\mathcal{T}) has long been considered crucial. However, in the second half of the 20th century, experimental evidence emerged confirming the violation of both \mathcal{P} and the combined \mathcal{CP} symmetries in weak interactions. Nowadays, the violation of \mathcal{CP} symmetry holds immense interest in the fields of cosmology and astrophysics because it is considered one of the three fundamental conditions for baryogenesis [1]. Consequently, the exploration of novel manifestations of symmetry violation has emerged as a prominent research area in contemporary theoretical and experimental physics [2].

One of the approaches used to explore these phenomena is by studying the electron electric dipole moment ($e\text{EDM}$) and nuclear magnetic quadrupole moments (MQM), which serve as highly sensitive probes for testing the boundaries of the standard model of electroweak interactions and its extensions [3–8]. The search for both $e\text{EDM}$ and MQM are now being extensively studied. Recently the group from the Joint Institute for Laboratory Astrophysics (JILA) has obtained a new constraint on the $e\text{EDM}$, $|d_e| < 4.1 \times 10^{-30}$ $e\text{ cm}$ (90% confidence) [9], using the $^{180}\text{Hf } ^{19}\text{F}^+$ ions trapped in a rotating electric field. It further improves the latest ACME Collaboration result obtained in 2018, $|d_e| \lesssim 1.1 \times$

10^{-29} $e\text{ cm}$ [10], by a factor of 2.4 and the first result $|d_e| \lesssim 1.3 \times 10^{-28}$ on the $^{180}\text{Hf } ^{19}\text{F}^+$ ions [11] by a factor of about 32. Planned experiments aiming to measure MQM with the use of molecules offer a pathway to investigate \mathcal{P}, \mathcal{T} -odd nuclear forces, quark chromo-EDMs, and other \mathcal{CP} -violating quark interactions [12].

In this paper, our focus is on the MQM of ^{175}Lu in the LuOH^+ molecular ion, specifically in the ground rotational level of the first-excited bending vibrational mode. The choice of LuOH^+ is motivated by its electronic-structure similarities to YbOH , while also demonstrating even higher sensitivity to nuclear \mathcal{CP} -violating effects due to the large electric quadrupole moment of ^{175}Lu [13].

In a polar molecule containing a heavy atom, the \mathcal{T}, \mathcal{P} -violating energy shifts induced by $e\text{EDM}$ and MQM are

$$\Delta E_{\mathcal{P}, \mathcal{T}} = P_e E_{\text{eff}} d_e + P_M W_M M, \quad (1)$$

where d_e is the value of the $e\text{EDM}$, M is the value of the MQM, factors E_{eff} and W_M are determined by the electronic structure of the molecule, P_e and P_M are the corresponding \mathcal{P}, \mathcal{T} -odd polarization coefficients.¹ To extract M and d_e from the measured energy shift $\Delta E_{\mathcal{P}, \mathcal{T}}$, one needs to know E_{eff} , W_M , P_e , and P_M . [15]. The value of W_M was calculated in Ref. [13], E_{eff} was calculated in Ref. [15]. An important task is to distinguish between the two sources of symmetry violation. This can be achieved by using different molecules or different

¹The polarization factors for both the electric dipole moment ($e\text{EDM}$) and the scalar \mathcal{T}, \mathcal{P} -odd electron-nucleus interaction effects are identical. For brevity, we only mention the $e\text{EDM}$ in this paper. To be precise, nuclei with a spin of $I \geq 1/2$ acquire a Schiff moment, which, similar to MQM, contributes to the nuclear-spin-dependent \mathcal{T}, \mathcal{P} -odd energy shift. However, in the case of open shells, there are reasons to believe that MQM can take precedence [14]. In this paper, we specifically focus on the effects of MQM.

*kurchavov_ip@pnpi.nrcki.ru

†daniel.majson@gmail.com; maison_de@pnpi.nrcki.ru

‡skripnikov_lv@pnpi.nrcki.ru; leonidos239@gmail.com

§mgrau@odu.edu

¶petrov_an@pnpi.nrcki.ru

electronic states of the same molecule. However, as can be seen from Eq. (1), it is also possible to utilize two or more sublevels of the same electronic state with different P_e/P_M ratios. Therefore, an accurate method for estimating these ratios is necessary. In Ref. [15], we calculated the value of P_e for $^{175}\text{Lu OH}^+$. In Ref. [16], a method for calculating P_M was developed and applied to the $^{173}\text{Yb OH}$ molecule. The main objective of this study is to apply this method to calculate P_M for $^{175}\text{Lu OH}^+$. Furthermore, more precise data for P_e , hyperfine structure, and spectroscopic constants are obtained.

II. METHODS

Following Ref. [17], we present the Hamiltonian in the molecular reference frame as follows:

$$\hat{\mathbf{H}} = \hat{\mathbf{H}}_{\text{mol}} + \hat{\mathbf{H}}_{\text{hfs}} + \hat{\mathbf{H}}_{\text{ext}}. \quad (2)$$

Two approaches for the molecular Hamiltonian $\hat{\mathbf{H}}_{\text{mol}}$ are used:

$$\hat{\mathbf{H}}_{\text{mol}}^{\text{I}} = \frac{(\hat{\mathbf{J}} - \hat{\mathbf{J}}^{e-v})^2}{2\mu R_e^2} + \frac{(\hat{\mathbf{J}}^v)^2}{2\mu_{\text{OH}} r^2} + V(R_e, \theta), \quad (3)$$

and

$$\hat{\mathbf{H}}_{\text{mol}}^{\text{II}} = -\frac{\hbar^2}{2\mu} \frac{\partial^2}{\partial R^2} + \frac{(\hat{\mathbf{J}} - \hat{\mathbf{J}}^{e-v})^2}{2\mu R^2} + \frac{(\hat{\mathbf{J}}^v)^2}{2\mu_{\text{OH}} r^2} + V(R, \theta), \quad (4)$$

where μ is the reduced mass of the Lu-OH system, μ_{OH} is the reduced mass of the OH, $\hat{\mathbf{J}}$ is the total electronic, vibrational, and rotational angular momentum, $\hat{\mathbf{J}}^{e-v} = \hat{\mathbf{J}}^e + \hat{\mathbf{J}}^v$ is the electronic-vibrational momentum, $\hat{\mathbf{J}}^e$ is the electronic momentum, $\hat{\mathbf{J}}^v$ is the vibrational momentum, R is the distance between Lu and the center mass of OH, $R_e = 1.930 \text{ \AA}$ is the corresponding equilibrium value for R , $r = 0.954 \text{ \AA}$ is OH bond length, θ is the angle between OH and the axis (z axis of the molecular frame) directed from Lu to the OH center of mass, and $V(R, \theta)$ is the potential-energy surface obtained in electronic structure calculations. The condition $\theta = 0$ corresponds to the linear configuration where the O nucleus is between the Lu and H nuclei. R , r , and θ are the so-called Jacobi coordinates,² see Fig. 1.

Using the Hamiltonian $\hat{\mathbf{H}}_{\text{mol}}^{\text{I}}$, we neglect the influence of the stretching ν_1 (associated with R) and OH ligand ν_3 (associated with r) vibrational modes. However, we still consider the bending modes ν_2 (associated with θ) with fixed R and r . In this approach, the spectroscopic constants and P_e coefficient were calculated in Ref. [15]. Using the Hamiltonian $\hat{\mathbf{H}}_{\text{mol}}^{\text{II}}$, we additionally take into account the influence of the stretching mode. In this work, we recalculated the spectroscopic constants (and obtained a new one for the stretching mode) and the P_e value using $\hat{\mathbf{H}}_{\text{mol}}^{\text{II}}$. Furthermore, we calculated the polarization P_M in both approaches.

²When defining Jacobi coordinates, the masses of the corresponding nuclei rather than atoms are used. So, for example, the Jacobi coordinates for the neutral LuOH molecule and the LuOH⁺ molecular cation are the same.

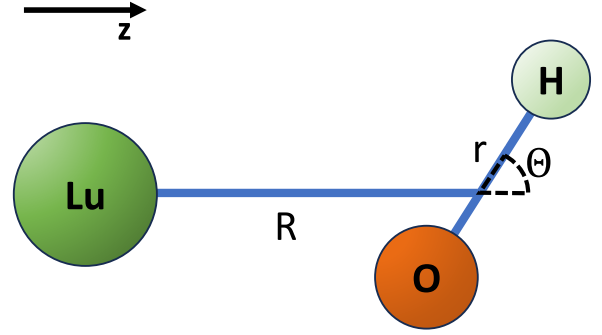


FIG. 1. The Jacobi coordinates for the LuOH⁺ cation are defined as follows: R is the distance between Lu and the center of mass of OH, while θ denotes the angle between the OH axis and the axis directed from Lu to the OH center of mass (the z axis of the molecular frame).

The Hamiltonian for the hyperfine interaction of electrons with Lu and H nuclei reads

$$\begin{aligned} \hat{\mathbf{H}}_{\text{hfs}} = & -g_{\text{H}} I^{\text{H}} \cdot \sum_a \left(\frac{\boldsymbol{\alpha}_{2a} \times \mathbf{r}_{2a}}{r_{2a}^3} \right) \\ & - g_{\text{Lu}} \mu_{\text{N}} I^{\text{Lu}} \cdot \sum_a \left(\frac{\boldsymbol{\alpha}_a \times \mathbf{r}_{1a}}{r_{1a}^3} \right) \\ & - e^2 \sum_q (-1)^q \hat{Q}_q^2(I^{\text{Lu}}) \sum_a \sqrt{\frac{2\pi}{5}} \frac{Y_{2q}(\theta_{1a}, \phi_{1a})}{r_{1a}^3}, \end{aligned} \quad (5)$$

where g_{Lu} and g_{H} are the g -factors of the lutetium and hydrogen nuclei, $\boldsymbol{\alpha}_a$ are the Dirac matrices for the a th electron, \mathbf{r}_{1a} and \mathbf{r}_{2a} are their radius vectors in the coordinate system centered on the Lu and H nuclei, $\hat{Q}_q^2(I^{\text{Lu}})$ is the quadrupole moment operator for ^{175}Lu nucleus, and $I^{\text{Lu}} = 7/2$, $I^{\text{H}} = 1/2$ are nuclear spins for ^{175}Lu and ^1H .

The Stark Hamiltonian

$$\hat{\mathbf{H}}_{\text{ext}} = -\mathbf{D} \cdot \mathbf{E} \quad (6)$$

describes the interaction of the molecule with the external electric field, and \mathbf{D} is the dipole-moment operator.

Wave functions, rovibrational energies, and hyperfine structure were obtained by numerically diagonalizing the Hamiltonian (2) over the basis set of electronic-rotational-vibrational-nuclear spins wave functions:

$$\Psi_{\Omega m \omega} P_{lm}(\theta) \Theta_{M_J, \omega}^J(\alpha, \beta) U_{M_I^{\text{H}}}^{\text{H}} U_{M_I^{\text{Lu}}}^{\text{Lu}}. \quad (7)$$

or

$$\Psi_{\Omega m \omega} \chi_{\nu_1}(R) P_{lm}(\theta) \Theta_{M_J, \omega}^J(\alpha, \beta) U_{M_I^{\text{H}}}^{\text{H}} U_{M_I^{\text{Lu}}}^{\text{Lu}}, \quad (8)$$

for $\hat{\mathbf{H}}_{\text{mol}}^{\text{I}}$ or $\hat{\mathbf{H}}_{\text{mol}}^{\text{II}}$, respectively. Here $\Theta_{M_J, \omega}^J(\alpha, \beta) = \sqrt{(2J+1)/4\pi} D_{M_J, \omega}^J(\alpha, \beta, \gamma=0)$ is the rotational wave function, $D_{M_J, \omega}^J$ is the Wigner function, α, β correspond to azimuthal and polar angles of the molecular z axis (directed from Lu to the center of mass of the OH group), respectively, $U_{M_I^{\text{H}}}^{\text{H}}$ and $U_{M_I^{\text{Lu}}}^{\text{Lu}}$ are the hydrogen and lutetium nuclear-spin wave functions, respectively, M_J is the projection of the molecular (electronic-rotational-vibrational) angular momentum $\hat{\mathbf{J}}$ on the laboratory axis, ω is the projection of

the same momentum on the z axis of the molecular frame, M_I^H and M_I^{Lu} are the projections of the nuclear angular momenta of hydrogen and lutetium on the laboratory axis, respectively, $P_l(\theta)$ is the associated Legendre polynomial, l is the vibration angular momentum and m is its projection on the molecular axis, Ω is the projection of the total electronic angular momentum on the molecular axis z for linear configuration. $\Psi_{\Omega m \omega}$ is the electronic wave function (see Ref. [17] for details).

In this calculation functions with $\omega - m = \Omega = \pm 1/2$, $l = 0 - 30$, and $m = 0, \pm 1, \pm 2$, $J = 1/2, 3/2, 5/2$ were included in the basis sets (7) and (8). The ground vibrational state $\nu_2 = 0$ corresponds to $m = 0$, the first-excited bending mode $\nu_2 = 1$ to $m = \pm 1$, the second excited bending mode has states with $m = 0, \pm 2$, etc. A common designation ν_2^m for the bending vibrational levels will be used below. The quantum number ν_1 is not associated with any momenta.

If the electronic-vibrational matrix elements are known, the matrix elements of \hat{H} between states in the basis set (8) can be calculated using angular-momentum algebra [17,18], similar to the approach used for diatomic molecules [19]. The relevant matrix elements are obtained from Ref. [15]. To calculate the \mathcal{T} , \mathcal{P} -odd shifts, the average value of the following Hamiltonians [20–22] were calculated [15]:

$$H_{MQM} = -\frac{M}{2I^{Lu}(2I^{Lu} - 1)} T_{ik} \frac{3}{2r^5} \epsilon_{jli} \alpha_j r_l r_k, \quad (9)$$

$$H_{EDM} = d_e 2ic \gamma^0 \gamma^5 \mathbf{p}^2, \quad (10)$$

where

$$T_{ik} = I_i^{Lu} I_k^{Lu} + I_k^{Lu} I_i^{Lu} - \frac{2}{3} \delta_{i,k} I^{Lu} (I^{Lu} + 1). \quad (11)$$

Here ϵ_{jli} is the unit antisymmetric tensor, $\boldsymbol{\alpha}$ is the vector of Dirac matrices, \mathbf{p} is the momentum operator for an electron and γ^0 and γ^5 are the Dirac matrices.

The potential-energy surface was calculated at three levels: self-consistent field (SCF), coupled cluster with single and double excitation amplitudes (CCSD), and coupled cluster with single, double, and perturbative triple excitation amplitudes [CCSD(T)]. These calculations were performed using the Dirac-Coulomb Hamiltonian. For Lu, we utilized the uncontracted Dyall's AE3Z basis set [23], while for F, we employed the aug-cc-PVTZ-DK basis set [24,25]. In the correlation calculations, we excluded the $1s \dots 3d$ electrons of Lu, and a cutoff for virtual orbital energy was set to 70 Hartree. Relativistic calculations were performed using the DIRAC19 code [26,27]. The one-electron functions used in the correlation calculations were obtained for the charged state of LuOH^{2+} . No approximations were made in the treatment of the small components (such as introduced in Ref. [28]) of molecular bispinors when calculating the primitive Coulomb integrals.

The potential-energy surface $V(R, \theta)$ was calculated using the following grid of coordinates (R_i, θ_k):

$$\{R_i\} = 1.771, 1.877, 1.930, 1.983, 2.089 \text{ \AA}, \quad (12)$$

$$\{\theta_k\} = 0^\circ, 5^\circ, 10^\circ, 15^\circ, 20^\circ, 25^\circ, 55^\circ, 90^\circ, 122^\circ, 155^\circ, 180^\circ. \quad (13)$$

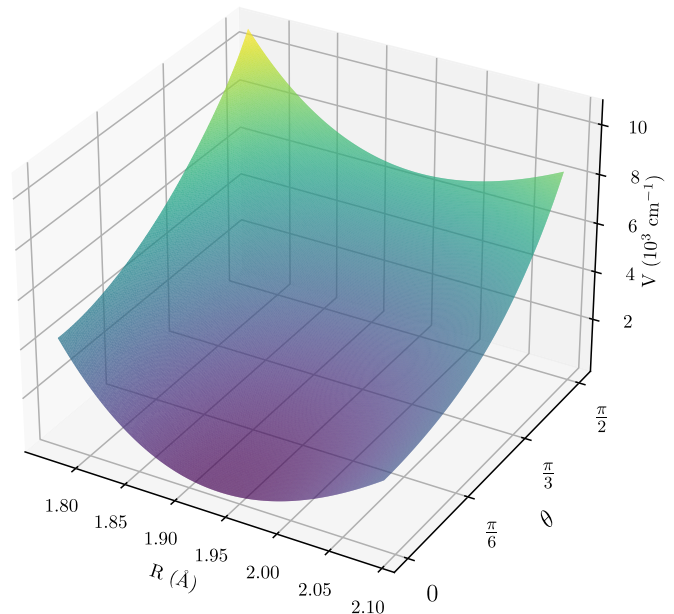


FIG. 2. The potential-energy surface $V(\theta, R)$ obtained at the CCSD(T) level and using polynomial interpolation. Data and fitting coefficients are available in the Supplemental Material.

Obtained potentials on the grid were approximated by a polynomial of the form $\sum_{n=0}^7 \sum_{m=0}^4 C_{nm} \theta^n R^m$. Since the minimum energy corresponds to the linear configuration, the coefficients $C_{nm} = 0$ for $n = 1$.

III. RESULTS AND DISCUSSIONS

Electronic structure calculations performed at the SCF, CCSD, and CCSD(T) levels give the linear equilibrium geometry for LuOH^+ corresponding to $\theta = 0$. The equilibrium value $r = 0.954 \text{ \AA}$, which was obtained at the CCSD(T) level, was fixed in other calculations. The equilibrium values $R = 1.944 \text{ \AA}$, $R = 1.928 \text{ \AA}$, and $R = 1.930 \text{ \AA}$ were obtained at the SCF, CCSD, and CCSD(T) levels, respectively. The corresponding Lu–O bond length $R_{\text{Lu-O}} = [1 - m_{(1\text{H})}/(m_{(16\text{O})} + m_{(1\text{H})})]R = 0.9407R$ is 1.829 \AA , 1.814 \AA , and 1.816 \AA for the SCF, CCSD, and CCSD(T) levels, respectively. Here $m_{(1\text{H})}$ and $m_{(16\text{O})}$ are the masses of ^1H and ^{16}O nuclei. As one can see, the inclusion of perturbative triple excitation amplitudes results in a change in the equilibrium geometry of less than 0.01 \AA . The latter value can be used as an estimate of the theoretical uncertainty of the equilibrium geometry parameters.

In Fig. 2 and Table I, we present the calculated potential-energy surface and spectroscopic properties. Data and fitting coefficients are available in Table S1 and Table S2 in the Supplemental Material [29]. With the exception of the stretching mode frequency ν_1 , the difference between the results obtained at the SCF and CCSD levels is much larger (approximately six times for the bending-mode frequencies and rotational constants, and about twenty times for the l doubling) than the difference between the CCSD and CCSD(T) results. It can be seen that the results for the CCSD and CCSD(T) models are in close agreement with each other. Incorporating the perturbative triple excitation amplitudes leads

TABLE I. Calculated vibrational energy levels (cm^{-1}), rotational constants B (cm^{-1}), and l doubling (MHz) for the excitation modes of stretching $\nu_1 = 0 - 1$ and bending $\nu_2 = 0 - 2$ quanta of $^{175}\text{Lu OH}^+$. Ligand mode ν_3 quanta is zero in calculations.

Parameter	CCSD(T)			
	(R frozen)	SCF	CCSD	CCSD(T)
$\nu_1 = 0, \nu_2 = 0$	0	0	0	0
$\nu_1 = 0, \nu_2 = 1$	442	460	438	434
$\nu_1 = 1, \nu_2 = 0$		745	750	745
$\nu_1 = 0, \nu_2 = 2^0$	871	905	864	856
$\nu_1 = 0, \nu_2 = 2^2$	898	931	887	880
$B(\nu_1 = 0, \nu_2 = 0)$	0.2879	0.2827	0.2874	0.2868
$B(\nu_1 = 0, \nu_2 = 1)$	0.2881	0.2823	0.2869	0.2863
$B(\nu_1 = 1, \nu_2 = 0)$		0.2815	0.2862	0.2855
$B(\nu_1 = 0, \nu_2 = 2^0)$	0.2883	0.2823	0.2870	0.2864
$B(\nu_1 = 0, \nu_2 = 2^2)$	0.2882	0.2871	0.2919	0.2912
$l\text{-ing}(\nu_1 = 0, \nu_2 = 1)$	23.5	22.6	24.4	24.5
$l\text{-ing}(\nu_1 = 0, \nu_2 = 2^2)$	0.005	0.010	0.012	0.012

to a decrease in vibrational energies by $4\text{--}8 \text{ cm}^{-1}$. The use of the Hamiltonian $\hat{H}_{\text{mol}}^{\text{II}}$ instead of $\hat{H}_{\text{mol}}^{\text{I}}$ has a slightly greater impact on the vibrational energies. The final l -doubling value for $\nu_2 = 1$ of 24.5 MHz is approximately 1 MHz higher than the value obtained with a frozen R variable.

Figure 3 gives the calculated polarizations P_e, P_M for the selected levels of the lowest $N = 1$ rotational state of the first-excited $\nu_2 = 1$ bending vibrational mode with frozen R

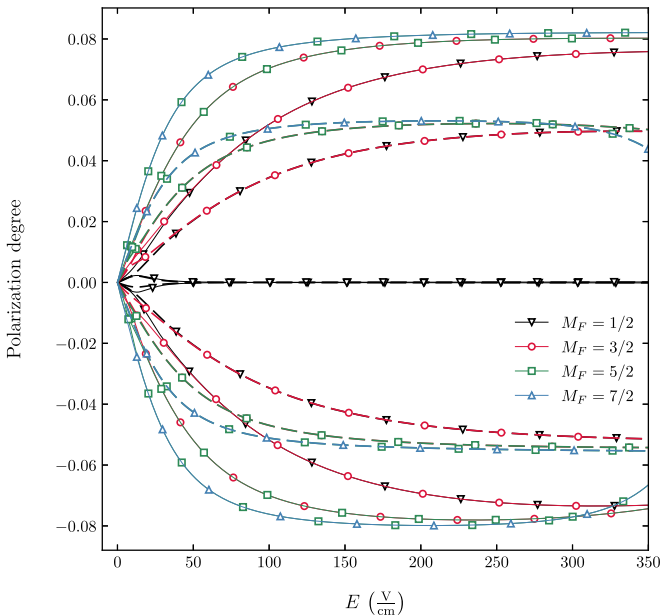


FIG. 3. Calculated polarizations $P_e/7$ (solid) and P_M (dashed) for the selected levels numbered 43–56 in Tables II and III (see text for details) for the different values of M_F of the lowest $N = 1$ rotational level of the first-excited $\nu_2 = 1$ bending vibrational mode of $^{175}\text{Lu OH}^+$ as functions of the external electric field. Since the influence of the hydrogen nuclear spin is very small, some curves for the states which differ by only projection $M_F^{\text{H}} = \pm 1/2$ coincide. It looks like the curves are labeled by two figures.

approximation as a functions of the external electric field. The selected 14 levels, numbered 43–56 (see Tables II and III), are those which were chosen in Ref. [15] for the $e\text{EDM}$ search. The corresponding energies (on the order of $31\,850 \text{ MHz}$) are given in Fig. 3(a) of Ref. [15]. Using only levels numbered 43–56 is not enough, however, if nonzero MQM of ^{175}Lu nucleus is assumed. The reason is that the ratio $P_e/P_M \approx -10.5$ is about the same for all these levels, which makes it impossible to distinguish $e\text{EDM}$ and MQM contributions. Similarly to P_e [15], there are levels with close values of P_M . These states differ by only projection $M_F^{\text{H}} = \pm 1/2$ which almost does not influence P_e and P_M .

The numerical data for P_e, P_M and hyperfine energies for all $N = 1$ levels for $E = 50$ and $E = 100 \text{ V/cm}$ are given in Tables II and III, respectively. To assess the influence of the stretching mode, calculations with Hamiltonians $\hat{H}_{\text{mol}}^{\text{I}}$ and $\hat{H}_{\text{mol}}^{\text{II}}$ were performed. One can see that accounting for stretching mode leads to a decreasing of notable P_e, P_M values up to about 5% for $E = 50$ and 4% for $E = 100$. This is explained by an increasing l -doubling value describing the energy difference between levels of opposite parity at zero electric field when the stretching mode is taken into account. Since the MQM-induced energy shift is proportional to P_M for the MQM searches the levels with large P_M values are preferred. Besides, to distinguish $e\text{EDM}$ and MQM contributions, the levels with different P_e/P_M ratios have to be used. As an example of the proposed $e\text{EDM}$ contribution exclusion scheme, let us consider the first and fifty-third levels for $E = 50 \text{ V/cm}$. For the first level we have $\delta E^1 = -0.3740E_{\text{eff}}d_e + 0.0794W_M M$; for the fifty-third level $\delta E^{53} = -0.3524E_{\text{eff}}d_e + 0.0333W_M M$. Then the combination $\delta E^1 - 1.0613\delta E^{53} = 0.044W_M M$ is independent of $e\text{EDM}$ and can be used for MQM extraction. Similarly, for the electric field $E = 100 \text{ V/cm}$, for example, one can choose levels numbered 1 (with $\delta E^1 = -0.4715E_{\text{eff}}d_e + 0.1001W_M M$ and a ratio $P_e/P_M \approx 4.71$) and 43 (with $\delta E^{43} = 0.5294E_{\text{eff}}d_e - 0.0502W_M M$ and the ratio equal to 10.55). Then the combination obtained is $1.1229\delta E^1 + \delta E^{43} = 0.0622W_M M$. We note also that our choice of the levels is only an example. On the base of Tables II and III and using the formulas

$$MW_M = \frac{1}{\Delta} (P_e^x \delta E^y - P_e^y \delta E^x),$$

$$\Delta = P_e^x P_M^y - P_e^y P_M^x, \quad (14)$$

one can choose alternative appropriate levels for the MQM search. Here x and y are numbers of chosen levels. Similarly, the $e\text{EDM}$ contribution can be determined.

An electric field $E = 100 \text{ V/cm}$ provides almost saturated values for P_e and P_M . As it was shown in Ref. [17] that in the l -doubling structure, the P value tends to reach half of the maximum value for molecules with Hund's case b . Calculations showed that all levels have polarizations $P_e < 0.58$ and $P_M < 0.12$.

To access these energy levels to perform the $e\text{EDM}$ and MQM precision measurement, trapped LuOH^+ ions are initially prepared in the ground rovibrational state by either optical pumping or quantum logic spectroscopy. From this point, either of the states in the pair necessary to distinguish the $e\text{EDM}$ from MQM can be populated by driving

TABLE II. The calculated energies (in MHz), polarizations for the different projections of the total angular momentum M_F of the lowest $N = 1$ rotational level of the first-excited $v = 1$ bending vibrational mode of $^{175}\text{LuOH}^+$ for the value of the external electric field $E = 50$ V/cm. Levels are numbered by the increasing energy. Zero energy level corresponds to the lowest energy of $N = 1$ states at zero electric field. Calculation with frozen R variable are marked by (f).

#	M_F	En(f)	En	P_e (f)	P_e	P_M (f)	P_M	#	M_F	En(f)	En	P_e (f)	P_e	P_M (f)	P_M
1	2.5	-5.5	-5.3	-0.3812	-0.3740	0.0809	0.0794	49	0.5	31851.8	31849.4	0.0014	0.0013	-0.0001	-0.0001
2	1.5	-5.3	-5.1	-0.3811	-0.3738	0.0809	0.0794	50	0.5	31873.7	31872.1	-0.0013	-0.0012	0.0001	0.0001
3	1.5	-1.7	-1.7	-0.2450	-0.2374	0.0520	0.0504	51	0.5	31874.6	31872.9	-0.2151	-0.2070	0.0204	-0.0195
4	0.5	-1.6	-1.6	-0.2436	-0.2359	0.0517	0.0501	52	1.5	31874.6	31872.9	-0.2164	-0.2082	0.0206	0.0197
5	0.5	-0.2	-0.2	-0.0013	-0.0013	0.0003	0.0003	53	1.5	31876.9	31875.2	-0.3631	-0.3524	0.0345	0.0333
6	0.5	23.3	24.3	0.0011	0.0011	-0.0002	-0.0002	54	2.5	31877.0	31875.2	-0.3631	-0.3524	0.0345	0.0333
7	1.5	24.9	25.8	0.2448	0.2372	-0.0520	-0.0503	55	2.5	31880.1	31878.3	-0.4457	-0.4355	0.0423	0.0411
8	0.5	25.0	25.9	0.2436	0.2360	-0.0517	-0.0501	56	3.5	31880.3	31878.4	-0.4457	-0.4355	0.0423	0.0411
9	2.5	28.7	29.5	0.3808	0.3736	-0.0808	-0.0793	57	4.5	32043.2	32042.7	0.3530	0.3435	-0.0477	-0.0475
10	1.5	28.9	29.7	0.3807	0.3734	-0.0808	-0.0793	58	5.5	32043.3	32042.9	0.3528	0.3433	-0.0477	-0.0475
11	4.5	118.7	119.3	-0.3374	-0.3333	0.0703	0.0694	59	3.5	32045.9	32045.4	0.3266	0.3165	-0.0442	-0.0437
12	3.5	118.9	119.5	-0.3374	-0.3333	0.0703	0.0694	60	4.5	32046.1	32045.5	0.3265	0.3164	-0.0442	-0.0437
13	3.5	122.2	122.8	-0.3040	-0.2987	0.0633	0.0622	61	2.5	32048.4	32047.8	0.2853	0.2750	-0.0386	-0.0380
14	2.5	122.4	122.9	-0.3039	-0.2986	0.0633	0.0622	62	3.5	32048.5	32048.0	0.2853	0.2750	-0.0386	-0.0380
15	2.5	125.3	125.8	-0.2452	-0.2391	0.0511	0.0498	63	1.5	32050.5	32049.9	0.2203	0.2108	-0.0298	-0.0291
16	1.5	125.4	125.9	-0.2449	-0.2387	0.0510	0.0497	64	2.5	32050.6	32050.0	0.2205	0.2111	-0.0298	-0.0292
17	1.5	127.5	127.9	-0.1446	-0.1396	0.0301	0.0291	65	0.5	32052.0	32051.3	0.1202	0.1141	-0.0162	-0.0158
18	0.5	127.5	127.9	-0.1419	-0.1368	0.0296	0.0285	66	1.5	32052.0	32051.4	0.1241	0.1179	-0.0168	-0.0163
19	0.5	128.4	128.7	-0.0024	-0.0025	0.0005	0.0005	67	0.5	32052.5	32051.8	0.0036	0.0036	-0.0005	-0.0005
20	0.5	151.7	153.1	0.0020	0.0021	-0.0004	-0.0004	68	0.5	32075.7	32075.9	-0.0035	-0.0035	0.0005	0.0005
21	1.5	152.6	153.9	0.1444	0.1394	-0.0301	-0.0290	69	0.5	32076.3	32076.5	-0.1200	-0.1139	0.0162	0.0158
22	0.5	152.6	154.0	0.1422	0.1371	-0.0296	-0.0286	70	1.5	32076.3	32076.5	-0.1238	-0.1177	0.0168	0.0163
23	2.5	154.8	156.1	0.2450	0.2388	-0.0510	-0.0497	71	1.5	32077.8	32077.9	-0.2198	-0.2103	0.0297	0.0291
24	1.5	154.9	156.2	0.2447	0.2385	-0.0510	-0.0497	72	2.5	32077.8	32078.0	-0.2201	-0.2106	0.0298	0.0291
25	3.5	158.0	159.2	0.3036	0.2984	-0.0632	-0.0621	73	2.5	32080.0	32080.1	-0.2847	-0.2743	0.0385	0.0379
26	2.5	158.1	159.3	0.3036	0.2983	-0.0632	-0.0621	74	3.5	32080.1	32080.2	-0.2847	-0.2743	0.0385	0.0379
27	4.5	161.7	162.8	0.3369	0.3329	-0.0702	-0.0693	75	3.5	32082.8	32082.8	-0.3257	-0.3156	0.0441	0.0437
28	3.5	161.9	163.0	0.3369	0.3328	-0.0702	-0.0693	76	4.5	32082.9	32083.0	-0.3256	-0.3155	0.0441	0.0437
29	2.5	688.8	689.0	0.0456	0.0440	-0.0091	-0.0088	77	4.5	32085.9	32085.9	-0.3520	-0.3424	0.0477	0.0474
30	3.5	688.8	689.1	0.0457	0.0440	-0.0091	-0.0088	78	5.5	32086.0	32086.1	-0.3518	-0.3422	0.0477	0.0474
31	1.5	689.4	689.6	0.0312	0.0300	-0.0062	-0.0060	79	4.5	32319.7	32315.5	0.0083	0.0120	0.0108	0.0112
32	2.5	689.4	689.7	0.0314	0.0302	-0.0063	-0.0061	80	3.5	32319.9	32315.6	0.0082	0.0119	0.0107	0.0111
33	0.5	689.7	690.0	0.0145	0.0138	-0.0029	-0.0028	81	3.5	32320.3	32316.1	0.0063	0.0092	0.0083	0.0086
34	1.5	689.8	690.0	0.0162	0.0156	-0.0032	-0.0031	82	2.5	32320.4	32316.2	0.0062	0.0089	0.0081	0.0084
35	0.5	689.9	690.1	0.0016	0.0015	-0.0003	-0.0003	83	2.5	32320.8	32316.5	0.0044	0.0064	0.0058	0.0060
36	0.5	713.4	714.6	-0.0063	-0.0063	0.0013	0.0013	84	1.5	32320.8	32316.5	0.0039	0.0057	0.0052	0.0054
37	1.5	713.5	714.7	-0.0195	-0.0192	0.0039	0.0038	85	0.5	32321.0	32316.7	0.0014	0.0020	0.0018	0.0019
38	0.5	713.5	714.7	-0.0099	-0.0093	0.0020	0.0019	86	1.5	32321.0	32316.8	0.0025	0.0036	0.0032	0.0034
39	1.5	713.6	714.8	-0.0285	-0.0270	0.0057	0.0054	87	0.5	32321.2	32316.9	0.0007	0.0011	0.0010	0.0010
40	2.5	713.6	714.8	-0.0331	-0.0322	0.0066	0.0064	88	4.5	32342.1	32338.3	-0.0069	-0.0105	-0.0107	-0.0111
41	2.5	713.7	714.9	-0.0450	-0.0431	0.0090	0.0086	89	3.5	32342.1	32338.3	-0.0056	-0.0085	-0.0086	-0.0089
42	3.5	713.8	715.0	-0.0463	-0.0446	0.0092	0.0089	90	2.5	32342.1	32338.3	-0.0041	-0.0062	-0.0062	-0.0065
43	2.5	31845.7	31843.5	0.4474	0.4374	-0.0426	-0.0414	91	1.5	32342.1	32338.3	-0.0025	-0.0038	-0.0038	-0.0039
44	3.5	31845.8	31843.6	0.4473	0.4373	-0.0426	-0.0414	92	0.5	32342.1	32338.3	-0.0008	-0.0013	-0.0013	-0.0013
45	1.5	31848.7	31846.4	0.3642	0.3536	-0.0347	-0.0335	93	3.5	32342.3	32338.5	-0.0066	-0.0101	-0.0103	-0.0107
46	2.5	31848.8	31846.5	0.3642	0.3536	-0.0347	-0.0335	94	2.5	32342.3	32338.5	-0.0049	-0.0074	-0.0075	-0.0078
47	0.5	31850.9	31848.6	0.2156	0.2075	-0.0205	-0.0196	95	1.5	32342.3	32338.5	-0.0030	-0.0045	-0.0046	-0.0047
48	1.5	31851.0	31848.7	0.2170	0.2089	-0.0206	-0.0198	96	0.5	32342.3	32338.5	-0.0010	-0.0015	-0.0015	-0.0016

a Raman transition using a pair of far-detuned infrared lasers with a difference frequency tuned to the energy of the desired state. As the pair of states with an opposite projection of $M_F^H = \pm 1/2$ are separated in frequency by several MHz they will be straightforward to resolve experimentally.

IV. CONCLUSION

We calculated spectroscopic constants for the lowest vibrational levels as well as the parity-violating polarization parameters P_e and P_M associated with energy shifts induced by $e\text{EDM}$ and MQM of ^{175}Lu in the first-excited bending

TABLE III. The calculated energies (in MHz), polarizations for the different projections of the total angular momentum M_F of the lowest $N = 1$ rotational level of the first-excited $v = 1$ bending vibrational mode of $^{175}\text{Lu OH}^+$ for the value of the external electric field $E = 100$ V/cm. Levels are numbered by the increasing energy. Zero energy level corresponds to the lowest energy of $N = 1$ states at zero electric field. Calculation with frozen R variable are marked by (f).

#	M_F	En(f)	En	P_e (f)	P_e	P_M (f)	P_M	#	M_F	En(f)	En	P_e (f)	P_e	P_M (f)	P_M
1	2.5	-16.2	-15.9	-0.4750	-0.4715	0.1009	0.1001	49	0.5	31850.8	31848.4	-0.0001	-0.0001	0.0000	0.0000
2	1.5	-16.0	-15.8	-0.4750	-0.4714	0.1009	0.1001	50	0.5	31872.6	31870.9	0.0002	0.0002	0.0000	0.0000
3	1.5	-6.2	-6.0	-0.3811	-0.3739	0.0809	0.0794	51	0.5	31875.8	31874.0	-0.3626	-0.3519	0.0345	0.0333
4	0.5	-6.1	-5.9	-0.3809	-0.3736	0.0809	0.0793	52	1.5	31875.8	31874.1	-0.3625	-0.3517	0.0345	0.0332
5	0.5	-0.9	-0.9	-0.0004	-0.0004	0.0001	0.0001	53	1.5	31882.8	31880.9	-0.4904	-0.4813	0.0466	0.0454
6	0.5	22.5	23.5	0.0004	0.0004	-0.0001	-0.0001	54	2.5	31882.8	31881.0	-0.4903	-0.4812	0.0466	0.0454
7	1.5	27.9	28.8	0.3807	0.3734	-0.0808	-0.0792	55	2.5	31891.1	31889.2	-0.5331	-0.5256	0.0506	0.0496
8	0.5	28.0	28.8	0.3804	0.3731	-0.0807	-0.0792	56	3.5	31891.2	31889.3	-0.5330	-0.5255	0.0506	0.0495
9	2.5	38.6	39.3	0.4741	0.4706	-0.1006	-0.0999	57	4.5	32026.8	32026.5	0.4008	0.3931	-0.0542	-0.0543
10	1.5	38.7	39.4	0.4741	0.4706	-0.1006	-0.0998	58	5.5	32027.0	32026.6	0.4006	0.3929	-0.0542	-0.0543
11	4.5	102.3	103.0	-0.3830	-0.3816	0.0798	0.0795	59	3.5	32033.0	32032.5	0.3896	0.3814	-0.0526	-0.0526
12	3.5	102.5	103.2	-0.3830	-0.3815	0.0798	0.0795	60	4.5	32033.1	32032.7	0.3894	0.3812	-0.0526	-0.0526
13	3.5	110.4	111.0	-0.3691	-0.3668	0.0769	0.0764	61	2.5	32039.0	32038.5	0.3692	0.3603	-0.0498	-0.0496
14	2.5	110.5	111.2	-0.3691	-0.3667	0.0769	0.0764	62	3.5	32039.1	32038.6	0.3691	0.3601	-0.0498	-0.0496
15	2.5	118.1	118.7	-0.3370	-0.3329	0.0702	0.0693	63	1.5	32044.6	32044.1	0.3258	0.3159	-0.0439	-0.0435
16	1.5	118.2	118.8	-0.3369	-0.3329	0.0702	0.0693	64	2.5	32044.7	32044.2	0.3257	0.3157	-0.0439	-0.0435
17	1.5	124.6	125.1	-0.2450	-0.2388	0.0510	0.0497	65	0.5	32049.2	32048.6	0.2201	0.2107	-0.0297	-0.0290
18	0.5	124.7	125.2	-0.2446	-0.2384	0.0509	0.0497	66	1.5	32049.2	32048.6	0.2203	0.2109	-0.0297	-0.0290
19	0.5	127.7	128.1	-0.0004	-0.0004	0.0001	0.0001	67	0.5	32051.2	32050.5	0.0002	0.0002	0.0000	0.0000
20	0.5	151.0	152.4	0.0003	0.0004	-0.0001	-0.0001	68	0.5	32074.1	32074.3	-0.0002	-0.0002	0.0000	0.0000
21	1.5	154.1	155.4	0.2448	0.2386	-0.0510	-0.0497	69	0.5	32076.2	32076.4	-0.2195	-0.2101	0.0296	0.0289
22	0.5	154.2	155.4	0.2444	0.2382	-0.0509	-0.0496	70	1.5	32076.3	32076.4	-0.2197	-0.2102	0.0296	0.0290
23	2.5	161.0	162.1	0.3365	0.3324	-0.0701	-0.0692	71	1.5	32081.2	32081.3	-0.3246	-0.3146	0.0438	0.0434
24	1.5	161.1	162.2	0.3364	0.3324	-0.0701	-0.0692	72	2.5	32081.3	32081.3	-0.3245	-0.3145	0.0438	0.0433
25	3.5	169.2	170.3	0.3684	0.3660	-0.0767	-0.0762	73	2.5	32087.6	32087.6	-0.3676	-0.3585	0.0496	0.0495
26	2.5	169.4	170.4	0.3683	0.3660	-0.0767	-0.0762	74	3.5	32087.7	32087.7	-0.3674	-0.3584	0.0496	0.0495
27	4.5	178.0	179.1	0.3821	0.3806	-0.0796	-0.0793	75	3.5	32094.7	32094.6	-0.3876	-0.3793	0.0524	0.0524
28	3.5	178.2	179.2	0.3821	0.3806	-0.0796	-0.0793	76	4.5	32094.8	32094.7	-0.3874	-0.3792	0.0524	0.0524
29	2.5	687.2	687.5	0.0794	0.0772	-0.0159	-0.0155	77	4.5	32102.1	32102.1	-0.3988	-0.3909	0.0540	0.0542
30	3.5	687.3	687.6	0.0794	0.0772	-0.0159	-0.0155	78	5.5	32102.3	32102.2	-0.3985	-0.3907	0.0541	0.0542
31	1.5	689.4	689.7	0.0585	0.0565	-0.0117	-0.0113	79	4.5	32318.7	32314.5	0.0150	0.0217	0.0190	0.0198
32	2.5	689.5	689.8	0.0585	0.0566	-0.0117	-0.0113	80	3.5	32318.9	32314.6	0.0150	0.0216	0.0190	0.0198
33	0.5	690.9	691.1	0.0311	0.0299	-0.0062	-0.0060	81	3.5	32320.9	32316.6	0.0119	0.0172	0.0154	0.0160
34	1.5	690.9	691.1	0.0315	0.0303	-0.0063	-0.0061	82	2.5	32321.0	32316.7	0.0118	0.0171	0.0153	0.0159
35	0.5	691.4	691.6	0.0003	0.0003	-0.0001	-0.0001	83	2.5	32322.4	32318.2	0.0083	0.0121	0.0109	0.0113
36	0.5	714.8	716.0	-0.0032	-0.0035	0.0006	0.0007	84	1.5	32322.5	32318.3	0.0082	0.0120	0.0108	0.0112
37	0.5	715.0	716.2	-0.0285	-0.0270	0.0057	0.0054	85	1.5	32323.4	32319.2	0.0043	0.0063	0.0057	0.0059
38	1.5	715.0	716.2	-0.0322	-0.0311	0.0064	0.0062	86	0.5	32323.4	32319.2	0.0040	0.0057	0.0052	0.0054
39	1.5	715.3	716.5	-0.0588	-0.0568	0.0117	0.0113	87	0.5	32323.8	32319.5	0.0003	0.0005	0.0004	0.0005
40	2.5	715.4	716.5	-0.0593	-0.0574	0.0118	0.0114	88	4.5	32344.1	32340.3	-0.0126	-0.0190	-0.0187	-0.0195
41	2.5	715.9	717.0	-0.0804	-0.0783	0.0160	0.0156	89	3.5	32344.3	32340.4	-0.0120	-0.0180	-0.0177	-0.0184
42	3.5	715.9	717.1	-0.0805	-0.0784	0.0161	0.0156	90	3.5	32344.4	32340.6	-0.0110	-0.0166	-0.0161	-0.0168
43	2.5	31833.7	31831.6	0.5366	0.5294	-0.0512	-0.0502	91	2.5	32344.4	32340.6	-0.0089	-0.0133	-0.0127	-0.0132
44	3.5	31833.8	31831.8	0.5365	0.5293	-0.0511	-0.0502	92	1.5	32344.4	32340.6	-0.0054	-0.0081	-0.0077	-0.0080
45	1.5	31841.2	31839.0	0.4928	0.4839	-0.0470	-0.0459	93	0.5	32344.5	32340.6	-0.0018	-0.0027	-0.0026	-0.0027
46	2.5	31841.3	31839.1	0.4927	0.4838	-0.0470	-0.0459	94	2.5	32344.6	32340.7	-0.0091	-0.0135	-0.0131	-0.0135
47	0.5	31847.7	31845.4	0.3638	0.3532	-0.0347	-0.0335	95	1.5	32344.6	32340.8	-0.0061	-0.0089	-0.0086	-0.0089
48	1.5	31847.7	31845.5	0.3637	0.3531	-0.0347	-0.0335	96	0.5	32344.7	32340.8	-0.0021	-0.0031	-0.0030	-0.0031

mode of the $^{175}\text{Lu OH}^+$ cation. We found that accounting for the stretching vibrational mode leads to an increase in the l -doubling value for the first-excited bending mode by approximately 4% (from 23.5 to 24.6 MHz) and a decrease of the sensitivity to $e\text{EDM}$ and MQM of ^{175}Lu by about

4%–5% for the electric field $E = 50$ – 100 V/cm. Based on the calculated P_e and P_M values, we determined the levels that are suitable for the MQM search. We also proposed an approach for distinguishing the contributions of the $e\text{EDM}$ and MQM effects to the experimentally measured energy shift.

ACKNOWLEDGMENTS

Electronic structure calculations have been carried out using computing resources of the federal collective usage center Complex for Simulation and Data Processing for Mega-science Facilities at National Research Centre “Kurchatov Institute” [30]. Electronic correlation calculation of

the potential-energy surface was supported by the Russian Science Foundation (Grant No. 19-72-10019-P [31]). Dirac-Hartree-Fock calculations were supported by Foundation for the Advancement of Theoretical Physics and Mathematics “BASIS” grant according to the Research Project No. 21-1-2-47-1.

- [1] A. D. Sakharov, *JETP Lett.* **5**, 24 (1967).
- [2] M. S. Safronova, D. Budker, D. DeMille, D. F. J. Kimball, A. Derevianko, and C. W. Clark, *Rev. Mod. Phys.* **90**, 025008 (2018).
- [3] R. Alarcon, J. Alexander, V. Anastassopoulos, T. Aoki, R. Baartman, S. Baeßler, L. Bartoszek, D. H. Beck, F. Bedeschi *et al.*, [arXiv:2203.08103](https://arxiv.org/abs/2203.08103).
- [4] T. Fukuyama, *Int. J. Mod. Phys. A* **27**, 1230015 (2012).
- [5] M. Pospelov and A. Ritz, *Phys. Rev. D* **89**, 056006 (2014).
- [6] Y. Yamaguchi and N. Yamanaka, *Phys. Rev. Lett.* **125**, 241802 (2020).
- [7] Y. Yamaguchi and N. Yamanaka, *Phys. Rev. D* **103**, 013001 (2021).
- [8] V. V. Flambaum, D. DeMille, and M. G. Kozlov, *Phys. Rev. Lett.* **113**, 103003 (2014).
- [9] T. S. Roussy, L. Caldwell, T. Wright, W. B. Cairncross, Y. Shagam, K. B. Ng, N. Schlossberger, S. Y. Park, A. Wang, J. Ye, and E. A. Cornell, *Science* **381**, 46 (2023).
- [10] V. Andreev, D. Ang, D. DeMille, J. Doyle, G. Gabrielse, J. Haefner, N. Hutzler, Z. Lasner, C. Meisner, B. O’Leary *et al.*, *Nature (London)* **562**, 355 (2018).
- [11] W. B. Cairncross, D. N. Gresh, M. Grau, K. C. Cossel, T. S. Roussy, Y. Ni, Y. Zhou, J. Ye, and E. A. Cornell, *Phys. Rev. Lett.* **119**, 153001 (2017).
- [12] L. V. Skripnikov, A. N. Petrov, A. V. Titov, and V. V. Flambaum, *Phys. Rev. Lett.* **113**, 263006 (2014).
- [13] D. E. Maison, L. V. Skripnikov, V. V. Flambaum, and M. Grau, *J. Chem. Phys.* **153**, 224302 (2020).
- [14] D. E. Maison, L. V. Skripnikov, and V. V. Flambaum, *Phys. Rev. A* **100**, 032514 (2019).
- [15] D. E. Maison, L. V. Skripnikov, G. Penyazkov, M. Grau, and A. N. Petrov, *Phys. Rev. A* **106**, 062827 (2022).
- [16] I. Kurchavov and A. Petrov, *Phys. Rev. A* **106**, 062806 (2022).
- [17] A. Petrov and A. Zakharova, *Phys. Rev. A* **105**, L050801 (2022).
- [18] L. D. Landau and E. M. Lifshitz, *Quantum Mechanics*, 3rd ed. (Pergamon, Oxford, 1977).
- [19] A. N. Petrov, *Phys. Rev. A* **83**, 024502 (2011).
- [20] M. G. Kozlov, V. I. Fomichev, Yu. Yu. Dmitriev, L. N. Labzovsky, and A. V. Titov, *J. Phys. B: At. Mol. Phys.* **20**, 4939 (1987).
- [21] A.-M. Mårtensson-Pendrill and P. Öster, *Phys. Scr.* **36**, 444 (1987).
- [22] E. Lindroth, B. W. Lynn, and P. G. H. Sandars, *J. Phys. B: At. Mol. Opt. Phys.* **22**, 559 (1989).
- [23] A. S. P. Gomes, K. G. Dyall, and L. Visscher, *Theor. Chem. Acta* **127**, 369 (2010).
- [24] T. H. Dunning, Jr, *J. Chem. Phys.* **90**, 1007 (1989).
- [25] R. A. Kendall, T. H. Dunning, Jr, and R. J. Harrison, *J. Chem. Phys.* **96**, 6796 (1992).
- [26] DIRAC, a relativistic *ab initio* electronic structure program, Release DIRAC19 (2019), written by A. S. P. Gomes, T. Saue, L. Visscher, H. J. Aa. Jensen, and R. Bast, with contributions from I. A. Aucar, V. Bakken, K. G. Dyall, S. Dubillard, U. Ekstroem, E. Eliav, T. Enevoldsen, E. Fasshauer, T. Fleig, O. Fossgaard, L. Halbert, E. D. Hedegaard, T. Helgaker, J. Henriksson, M. Ilias, Ch. R. Jacob, S. Knecht, S. Komorovsky, O. Kullie, J. K. Laerdahl, C. V. Larsen, Y. S. Lee, H. S. Nataraj, M. K. Nayak, P. Norman, M. Olejniczak, J. Olsen, J. M. H. Olsen, Y. C. Park, J. K. Pedersen, M. Pernpointner, R. Di Remigio, K. Ruud, P. Salek, B. Schimmelpfennig, B. Senjean, A. Shee, J. Sikkema, A. J. Thorvaldsen, J. Thyssen, J. van Stralen, M. L. Vidal, S. Villaume, O. Visser, T. Winther, and S. Yamamoto, see <http://diracprogram.org>.
- [27] T. Saue, R. Bast, A. S. P. Gomes, H. J. A. Jensen, L. Visscher, I. A. Aucar, R. Di Remigio, K. G. Dyall, E. Eliav, E. Fasshauer, T. Fleig, L. Halbert, E. D. Hedegaard, B. Helmich-Paris, M. Ilias, C. R. Jacob, S. Knecht, J. K. Laerdahl, M. L. Vidal, M. K. Nayak *et al.*, *J. Chem. Phys.* **152**, 204104 (2020).
- [28] L. Visscher, *Theor. Chem. Acta* **98**, 68 (1997).
- [29] See Supplemental Material at <http://link.aps.org/supplemental/10.1103/PhysRevA.108.052815> for text file Supplementary.txt which contains data and fitting coefficients for the potential-energy surface.
- [30] <http://ckp.nrcki.ru/>
- [31] <https://rscf.ru/en/project/22-72-41010/>